





# The Role of IFITM Proteins in Tick-Borne Encephalitis Virus Infection

 Alicja M. Chmielewska,<sup>a</sup> Maria Gómez-Herranz,<sup>b,g</sup> Paulina Gach,<sup>a</sup> Marta Nekulova,<sup>c</sup>  Małgorzata A. Bagnucka,<sup>a</sup> Andrea D. Lipińska,<sup>a</sup> Michał Rychłowski,<sup>a</sup> Weronika Hoffmann,<sup>a</sup> Ewelina Król,<sup>d</sup> Borivoj Vojtesek,<sup>c</sup> Richard D. Sloan,<sup>e,f</sup> Krystyna Bieńkowska-Szewczyk,<sup>a</sup> Ted Hupp,<sup>b,g</sup> Kathryn Ball<sup>g</sup>

<sup>a</sup>Laboratory of Virus Molecular Biology, Intercollegiate Faculty of Biotechnology, University of Gdansk and Medical University of Gdańsk, Gdansk, Poland

<sup>b</sup>International Centre for Cancer Vaccine Science, University of Gdańsk, Gdansk, Poland

<sup>c</sup>Research Centre for Applied Molecular Oncology, Masaryk Memorial Cancer Institute, Brno, Czech Republic

<sup>d</sup>Laboratory of Recombinant Vaccines, Intercollegiate Faculty of Biotechnology, University of Gdańsk, Gdansk and Medical University of Gdańsk, Poland

<sup>e</sup>Infection Medicine, School of Biomedical Sciences, University of Edinburgh, Edinburgh, UK

<sup>f</sup>ZJU-UoE Institute, Zhejiang University, Haining, Zhejiang, People's Republic of China

<sup>g</sup>Institute of Genetics and Molecular Medicine, University of Edinburgh, Edinburgh, UK

Alicja M. Chmielewska and Maria Gómez-Herranz contributed equally to this article. The order of names of first authors was determined alphabetically.

**ABSTRACT** Tick-borne encephalitis virus (TBEV), of the genus *Flavivirus*, is a causative agent of severe encephalitis in regions of endemicity of northern Asia and central and northern Europe. Interferon-induced transmembrane proteins (IFITMs) are restriction factors that inhibit the replication cycles of numerous viruses, including flaviviruses such as West Nile virus, dengue virus, and Zika virus. Here, we demonstrate the role of IFITM1, IFITM2, and IFITM3 in the inhibition of TBEV infection and in protection against virus-induced cell death. We show that the most significant role is that of IFITM3, including the dissection of its functional motifs by mutagenesis. Furthermore, through the use of CRISPR-Cas9-generated IFITM1/3-knockout monoclonal cell lines, we confirm the role and additive action of endogenous IFITMs in TBEV suppression. However, the results of coculture assays suggest that TBEV might partially escape interferon- and IFITM-mediated suppression during high-density coculture infection when the virus enters naive cells directly from infected donor cells. Thus, cell-to-cell spread may constitute a strategy for virus escape from innate host defenses.

**IMPORTANCE** TBEV infection may result in encephalitis, chronic illness, or death. TBEV is endemic in northern Asia and Europe; however, due to climate change, new centers of endemicity have arisen. Although effective TBEV vaccines have been approved, vaccination coverage is low, and due to the lack of specific therapeutics, infected individuals depend on their immune responses to control the infection. IFITM proteins are components of the innate antiviral defenses that suppress cell entry of many viral pathogens. However, no studies on the role of IFITM proteins in TBEV infection have been published thus far. Understanding antiviral innate immune responses is crucial for the future development of antiviral strategies. Here, we show the important role of IFITM proteins in the inhibition of TBEV infection and virus-mediated cell death. However, our data suggest that TBEV cell-to-cell spread may be less prone to both interferon- and IFITM-mediated suppression, potentially facilitating escape from IFITM-mediated immunity.

**KEYWORDS** TBEV, IFITM, interferon, flavivirus, cell-to-cell spread, host factors, intrinsic immunity

**V**ector-borne flaviviruses, including tick-borne encephalitis virus (TBEV), West Nile virus, and dengue virus, cause millions of infections in humans worldwide. TBEV is transmitted to thousands of humans every year by tick bites or, occasionally, through infected milk

**Editor** Bryan R. G. Williams, Hudson Institute of Medical Research

**Copyright** © 2022 American Society for Microbiology. All Rights Reserved.

Address correspondence to Alicja M. Chmielewska, alicja.chmielewska@ug.edu.pl.

**Received** 5 July 2021

**Accepted** 2 October 2021

**Accepted manuscript posted online** 6 October 2021

**Published** 12 January 2022

(1). TBEV is endemic in northern Asia and central and northern Europe; however, as global climate change influences the distribution of ticks, new centers of endemicity have arisen (2–4). TBEV infects the central nervous system, with clinical outcomes ranging from mild meningitis to severe meningoencephalitis and paralysis (5). Depending on the virus subtype, the mortality rate ranges from 0.5 to 30% (6). Although several effective TBEV vaccines have been approved, vaccination coverage is low in some countries of endemicity; e.g., vaccination coverage is <15% in Germany and eastern Europe. Moreover, full protection is not acquired in some cases (7–9). Due to the lack of therapeutics for tick-borne encephalitis, treatment is symptomatic, and infected individuals depend on their innate and adaptive immune responses to fight the infection. Thus, in addition to prevention, an effective treatment is urgently needed (1).

TBEV is a 50-nm, single-positive-stranded RNA virus of the *Flaviviridae* family. Its 11-kb genome encodes a single polyprotein that is processed into 11 structural and nonstructural proteins (10–12). The TBEV nucleocapsid is surrounded by a bilayer envelope formed by host-originated lipids in which heterodimers made of envelope glycoprotein (E) and membrane protein (M) are embedded (13).

Flaviviruses are known to use a range of cellular attachment factors and receptors with some degree of overlap between them (14). Most flaviviruses use receptor-mediated endocytosis to achieve entry into cells, but dengue virus may also be able to use micropinocytosis (15). More specifically, TBEV is known to use heparin sulfate as an attachment factor (16) with laminin-binding protein (LBP) and the  $\alpha V\beta 3$  integrin as potential receptors (17). Alternatively, pH-dependent endosomal entry is another likely route due to the presence of histidine residues in the E protein of the virus susceptible to protonation which likely drive the conformational changes needed to achieve virus-cell membrane fusion (12).

The first line of antiviral defense is governed by innate immune responses. After recognition of a virus by pathogen recognition receptors (PRRs), a signaling cascade is triggered, resulting in the expression of inflammatory cytokines, such as type I interferon (IFN). IFN induces the expression of hundreds of IFN-stimulated genes (ISGs) that execute direct antiviral actions. IFN-induced transmembrane proteins (IFITMs) are important antiviral factors induced by IFN signaling (18, 19). The immune-related IFITM1, IFITM2, and IFITM3 are capable of attenuating the entry of a wide range of viruses, e.g., influenza A virus (IAV), human immunodeficiency virus type 1 (HIV-1), flaviviruses, filoviruses, and alphaviruses, and they modulate the entry of some coronaviruses, including severe acute respiratory syndrome coronavirus 2 (SARS-CoV-2), for which opposing activities of IFITMs have been reported (20–26). The scientific consensus is that IFITMs inhibit the cytosolic entry of viruses by preventing fusion of viral and host membranes, although there are reports describing their role in driving the production of virions of reduced infectivity or affecting the translation of viral proteins (27–29).

The IFN response is crucial in the host defense against TBEV. It has been shown that a local type I IFN response within the central nervous system is critical for the protection of mice against TBEV and other insect-borne flavivirus infections, including Zika virus (30–32). In addition, it has been shown that tick-borne flaviviruses are able to antagonize IFN signaling, resulting in their evasion from the host's innate immune system (33). Specifically, TBEV suppresses the Janus Kinase/Signal Transducer and Activator of Transcription (JAK/STAT) signaling cascade via NS5-mediated inhibition of STAT-1 phosphorylation (34). However, the effects of IFITM proteins on TBEV have not been investigated so far. Since IFITM2/3 are found and act predominantly in endosomes, restriction of TBEV by them in this location is entirely possible but remains unconfirmed (35). Notably, there are also variable reports regarding hepatitis C virus (HCV) susceptibility to IFITM proteins. IFITM1/2/3 were described to limit HCV entry in some studies (21, 36), while others noted that IFITM1 could not restrict entry into Huh7 cells but did restrict viral replication steps downstream of virus entry (37).

Here, we show that the IFITM1/2/3 proteins have the ability to suppress TBEV infection and protect cells against TBEV-induced death. We developed CRISPR–Cas9-generated IFITM1/3-knockout monoclonal cell lines, which allowed us to confirm the role of endogenous IFITMs in the inhibition of TBEV infection. Furthermore, we identified IFITM3 motifs that are crucial for

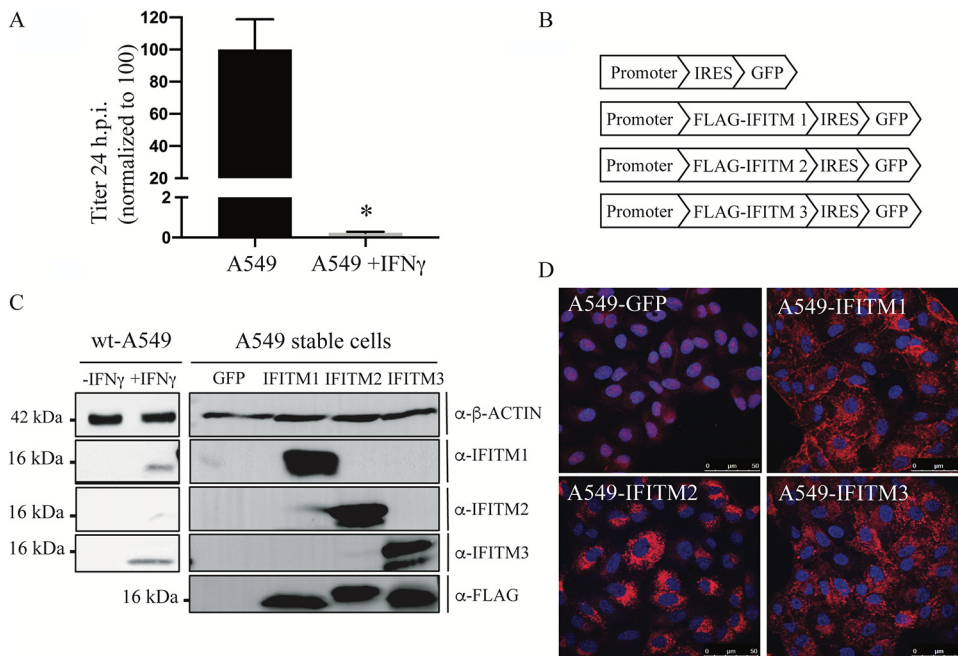


**FIG 1** Establishment of stable IFITM1/2/3-A549 cell lines to study their role in the restriction of TBEV infection. (A) A549 cells were infected for 24 h with TBEV at an MOI of 1. The virus titer decreased by  $>2$ -log fold with 100 ng/ml IFN- $\gamma$  stimulation for 24 h. Values indicate the means of  $n = 3$  independent experiments  $\pm$  the standard deviations (SD). \*,  $P = 0.01$  to  $0.05$  (Student  $t$  test). (B) Schematic of the constructs used to create stable IFITM-A549 cell lines expressing FLAG-tagged IFITM (IFITM1, IFITM2, or IFITM3) and then GFP. The control expressed only GFP. (C) The IFN- $\gamma$ -stimulated A549 cells and A549 cells stably expressing IFITM1/2/3 or empty cassettes were lysed, separated using SDS-PAGE, blotted, and stained with specific anti-IFITM antibodies or mouse monoclonal anti-FLAG antibodies.  $\beta$ -Actin was used as a protein loading control. (D) The expression of IFITM proteins in stably transduced A549 cells from panel C was analyzed by immunofluorescence using mouse monoclonal anti-FLAG antibody, followed by Alexa 546-conjugated anti-mouse IgG.

its anti-TBEV functions. Our results also show that cell-to-cell TBEV transmission is less sensitive to IFITM-mediated inhibition and IFN suppression than cell-free infection.

## RESULTS

**Evaluation of IFITM expression in wild-type and stably transduced A549 cell lines.** The goal of our study was to investigate and characterize the role of IFITM proteins in TBEV infection. Initially, we tested whether IFN- $\gamma$  inhibits TBEV infection in A549 lung epithelial cells. We found that A549 stimulation with IFN- $\gamma$  potentially inhibited the TBEV infection cycle and led to a reduction in the progeny virus titer by more than 2-log fold (Fig. 1A). To determine the role of each of IFITM protein in TBEV infection, we generated stable polyclonal A549 cell lines that expressed N-terminally FLAG-tagged IFITM1, IFITM2, or IFITM3, followed by a green fluorescent protein (GFP) sequence downstream from the internal ribosomal entry site (IRES), as well as a control cell line that expressed only GFP (Fig. 1B). We detected single bands and similar expression in all tagged IFITM proteins by Western blotting with an anti-FLAG antibody. However, we obtained double bands for all IFITM proteins with specific anti-IFITM1/2/3 antibodies, suggesting the presence of truncated IFITM species possibly lacking some N-terminal residues due to proteolysis or alternative translation start sites (Fig. 1C). The level of overexpressed IFITM proteins in the transduced cell lines was substantially higher than in the IFN- $\gamma$ -stimulated wild-type A549 cells, where we only detected signals for the IFITM1 and IFITM3 proteins (Fig. 1C). Nonstimulated A549 cells did not express detectable levels of endogenous IFITM proteins in the Western blot assay (Fig. 1C). Moreover, through immunofluorescence with an anti-FLAG antibody, we confirmed that the vast majority of the generated cells overexpressed IFITM proteins (Fig. 1D).

**IFITM1, IFITM2, and IFITM3 restrict TBEV infection.** To characterize the relative impacts of IFITM1, IFITM2, and IFITM3 on TBEV infection, we performed a TBEV infection assay at a

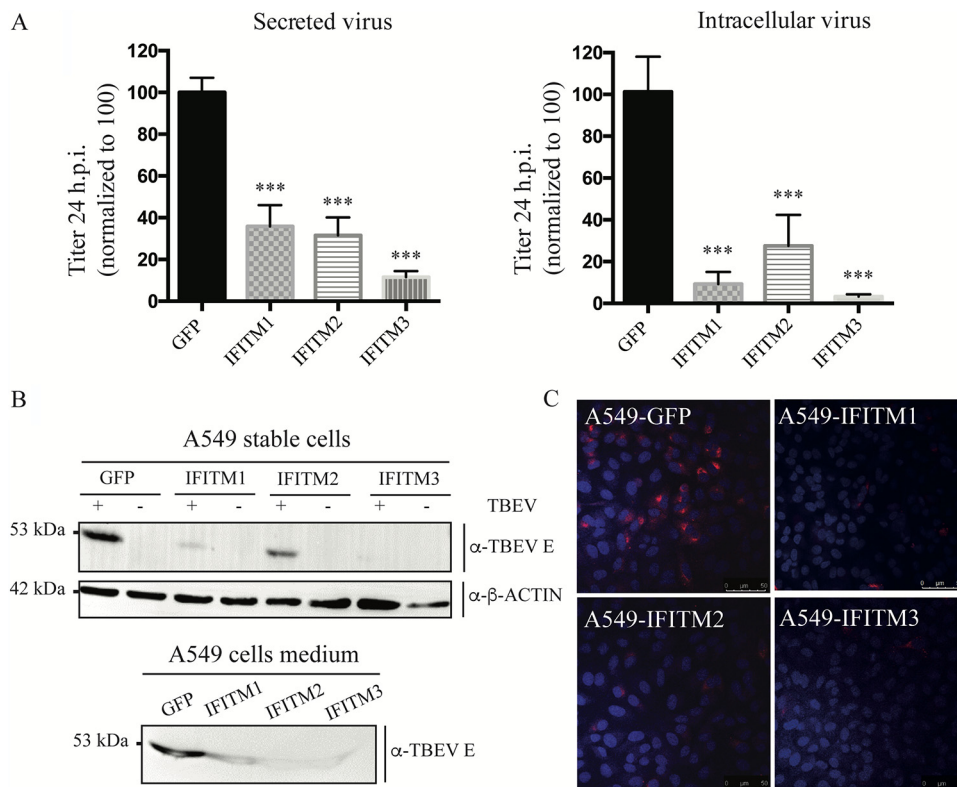


**FIG 2** IFITM1/2/3 proteins inhibit TBEV infection. A549 cells stably expressing IFITM1/2/3 or only GFP were plated in equal quantities and infected with TBEV virus of the Neudorf strain after 24 h at an MOI of 1 for 24 h. (A) Titers for media collected from cells and freeze-thawed cell lysates were determined using a plaque assay on wild-type A549 cells. Values indicate the means of  $n = 3$  independent experiments  $\pm$  the SD. \*\*\*,  $P < 0.001$  (Student *t* test). (B) Cell lysates and proteins precipitated from the medium of cells were separated using SDS-PAGE and analyzed by Western blotting with TBEV E antibody.  $\beta$ -Actin was used as a protein loading control. (C) The cells were fixed, stained with TBEV E antibody and DAPI, and analyzed using a Leica SP8X confocal laser scanning microscope.

multiplicity of infection (MOI) of 1. After 24 h, the media from the infected stable A549-IFITM1/2/3 cell lines and the A549-GFP control cells were collected and centrifuged. The cells were washed, covered with fresh medium, and lysed by freeze-thawing to liberate the intracellular viral particles. We analyzed the virus titer in the collected medium and cell lysates using a standard plaque assay. We demonstrated that, compared to A549-GFP cells, overexpression of IFITM1, IFITM2, and IFITM3 in A549 cells resulted in significant decreases in the TBEV titer by 92, 68, and 97%, respectively, for the intracellular virus and by 64, 68, and 88% for the medium-secreted virus (Fig. 2A). In addition, we detected substantially reduced levels of TBEV protein E in the cell lysates and proteins precipitated from the medium from A549 IFITM cells, with A549 IFITM3 showing the strongest reduction (Fig. 2B). This observation was further confirmed by immunofluorescence analysis of fixed and permeabilized cells that were stained with anti-E antibody. The percentage of E-protein-stained cells was substantially lower for all IFITM-overexpressing lines, and the fewest positive cells were found for the overexpression of IFITM3 (Fig. 2C).

**IFITM expression and TBEV restriction in A549-IFITM1/3-KO cells.** In order to investigate the antiviral activity of the IFITM proteins that were endogenously expressed in the A549 cells, we employed the CRISPR-Cas9 gene-editing methodology to generate A549 IFITM knockout cell lines. Based on the fact that for IFN- $\gamma$ -stimulated A549 cells, we were able to detect IFITM1 and IFITM3, but not IFITM2 (Fig. 1C), we developed a panel of monoclonal A549 cell lines with single knockouts (A549-IFITM1-KO and A549-IFITM3-KO) and with a double knockout (A549-IFITM1/IFITM3-KO). Single-guide RNAs (sgRNAs) were designed to target the N termini of IFITM1 and IFITM3. We then used a lentivirus transduction system to deliver distinct sgRNAs to wild-type A549

cells and applied selection pressure with puromycin. Individual cells were propagated, and cell clones were screened by Western blotting to identify clones with reduced or nondetectable IFITM1 and/or IFITM3 protein expression. Since we did not have an anti-IFITM1 antibody compatible with Western blotting at the time of the study, we immunoprecipitated IFITM1 using rabbit anti-IFITM1 serum (CVY) to screen A549-IFITM1-KO clones and then detected the precipitated IFITM1 using MHK2.1 antibody recognizing both IFITM1 and IFITM3 proteins. MHK2.1 was also used to screen A549-IFITM1/3-KO individual clones. To screen A549-IFITM3-KO individual clones, anti-IFITM3 antibody (Cell Signaling) was used. In Fig. 3A, the clones highlighted in red were used to study TBEV infection: A549-IFITM1-KO (clones 22 and 34), A549-IFITM3-KO (clones 5, 26, and 34), and A549-IFITM1/3-KO (clone 43).

To evaluate the susceptibility of the knockout cell lines to the virus, we performed a TBEV infection assay involving 24 h infection at an MOI of 1 and determined the percentage of cells that expressed TBEV E using flow cytometry (Fig. 3B). Reduced expression of IFITM1 or IFITM3 resulted in a significantly increased number of TBEV-positive cells. Interestingly, we obtained some variability in virus infections in different cell clones, which could be a result of either the gene-editing efficiency of CRISPR-Cas9 or other clone-related factors.

The single clone with the double IFITM1/IFITM3 knockout showed the highest (>8-fold) increase in virus susceptibility compared to the wild-type A549 cells. The cumulative effect of both IFITM1 and IFITM3 knockouts suggests that they restrict TBEV in a cooperative manner. The fact that nonstimulated IFITM1/3 knockout cell lines were more susceptible to TBEV infection than wild-type A549 cells coordinates with the observation that TBEV infection *per se* stimulated expression of IFITM1 and IFITM3 proteins in wild-type A549 cells (Fig. 3C). In summary, our experiments indicate that knocking out cellular IFITM1 and/or IFITM3 proteins in A549 facilitates TBEV infection, whereas ectopically overexpressed IFITM1/2/3 proteins effectively restrict TBEV infection *in vitro*.

**Important IFITM3 motifs required for the restriction of TBEV infection.** Previous studies focusing on IFITM3 restriction have indicated that IFITMs are heavily regulated by posttranslational modifications (PTMs), including phosphorylation, palmitoylation, ubiquitination, and methylation (38). In addition, IFITM3 forms homo- and hetero-oligomers that have been shown to depend on residues F75 and F78. The F75A/F78A mutations failed to inhibit IAV infection and showed mixed activity for coronaviruses (39, 40). In addition, the N-terminal domain of IFITM3 has been determined to be significant for antiviral activity against IAV but not against HIV-1 (41), whereas for IFITM2 with an N-terminal 21-amino-acid (aa) deletion, HIV-1 restriction was strain dependent (42). Moreover, the tyrosine residue Y20, which is a part of the phosphorylation motif present within the N-terminal domain, has been shown to determine cellular localization and antiviral activity against the influenza A and dengue viruses (39, 41).

To identify the determinants of IFITM3 function in TBEV infection, we generated polyclonal stable A549 cell lines that overexpressed mutated IFITM3 proteins, including mutations at specific posttranslational modification sites and deletions in the N-terminal region. To investigate the role of phosphorylation of IFITM3 in its antiviral actions against TBEV, we mutated tyrosine residues at positions 20 and 99 (Y20A and Y99A) and, for the analysis of palmitoylation, we mutated cysteine residues at positions 71 and 72 (C71A and C72A) of the FLAG-tagged IFITM3 sequence (Fig. 4A). To investigate the role of the F75 and F78 residues, which were previously determined to be crucial for IFITM3 oligomerization, we introduced a double phenylalanine-to-alanine mutation (FF75/78AA) in the FLAG-tagged IFITM3 sequence (Fig. 4A). In addition, we generated N-terminal IFITM3 mutants with a deletion of the first 21 aa ( $\Delta$ 21N) and short deletions in the N-terminal region ( $\Delta$ PVNSG and  $\Delta$ NSGQPP) (Fig. 4A). N-terminal mutants were generated on the basis of the nontagged IFITM3 sequence, since we anticipated that an N-terminal tag could interfere with function analysis of the N-terminal region. We assessed the level of mutated proteins in the cell extracts by Western blotting with an



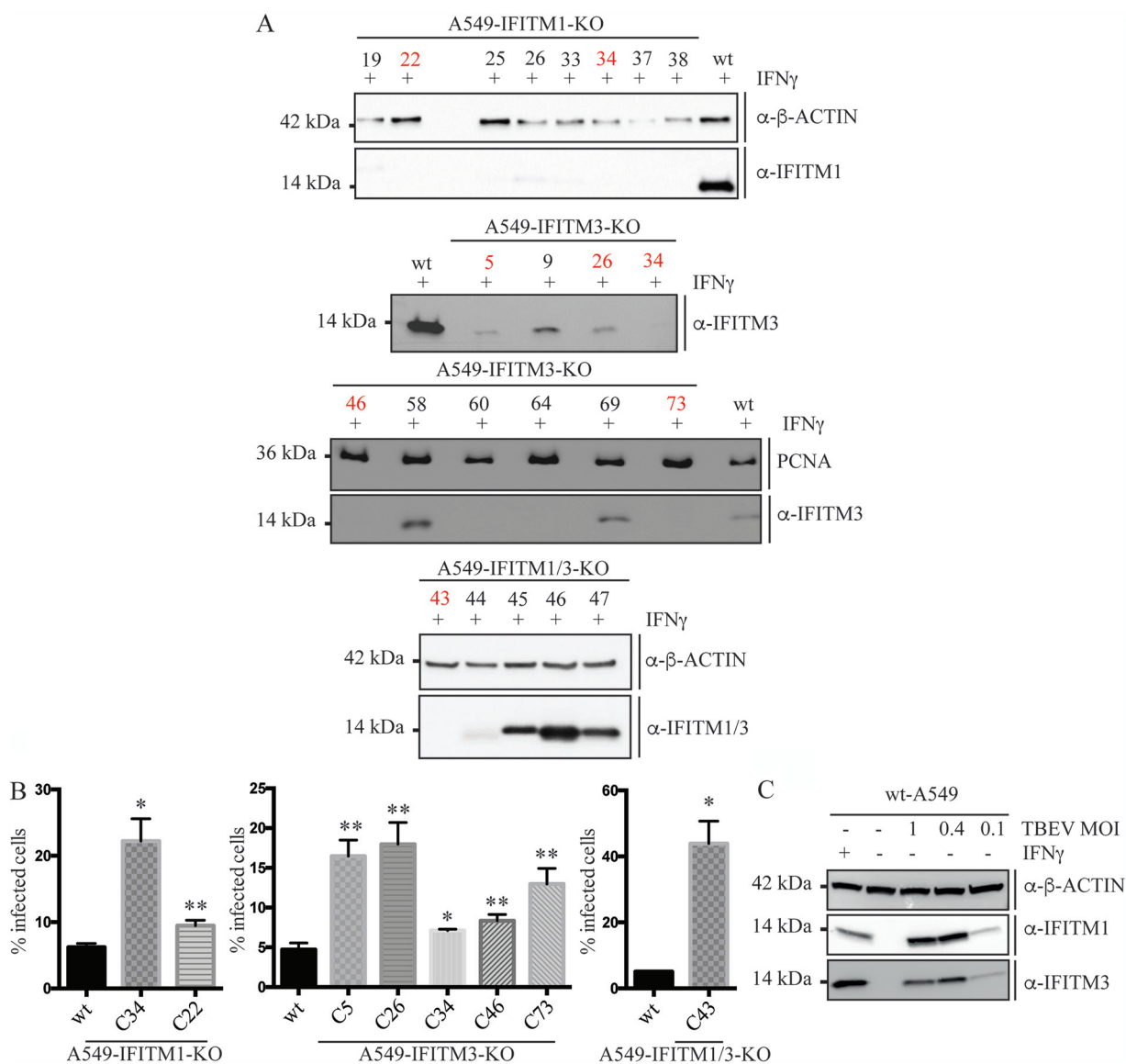


**FIG 3** Screening of A549-IFITM1-KO, A549-IFITM3-KO, and A549-IFITM1/3-KO cells and their effects on TBEV restriction. (A) Generation of IFITM knockouts in A549 cells by implementing CRISPR-Cas9 technology. Individual candidate clones were stimulated with 100 ng/ml IFN- $\gamma$ , screened by Western blotting to identify A549-IFITM1-KO, A549-IFITM3-KO, and A549-IFITM1/3-KO cells. The top panel shows the test of the loss of IFITM1 expression; IFITM1 was immunoprecipitated using rabbit anti-IFITM1 (CVY) antibody and tested with IFITM1/3 antibody MHK2.1 by Western blotting.  $\beta$ -Actin was used as a protein loading control. The A549-IFITM1-KO clones 22 and 34 were used in TBEV infection assay. The two panels in the middle demonstrate the loss of IFITM3 expression by Western blotting using IFITM3 antibody (Cell Signaling). PCNA (proliferating nuclear cell antigen) was used as a protein loading control. The A549-IFITM3-KO clones 5, 26, 34, 46, and 73 were used in TBEV infection assay. The lower panel shows the test of the loss of IFITM1/3 expression by Western blotting with an IFITM1/3 antibody MHK2.1.  $\beta$ -Actin was used as a protein loading control. The A549-IFITM1/3-KO clone 43 was used in TBEV infection assay. Molecular weights of IFITM proteins: IFITM1, 14 kDa; IFITM2 and IFITM3, 15 kDa. (B) The wild-type A549 cells and the different clones (highlighted in red) of IFITM1 and/or IFITM3 knockout cells were plated in equal quantities and, after 24 h, they were infected with TBEV of the Neudorf strain at an MOI of 0.1. At 24 hpi, the cells were stained with TBEV E antibody and analyzed by flow cytometry. Values indicate the mean of  $n = 3$  independent experiments  $\pm$  the SD. \*,  $P = 0.01$  to  $0.05$ ; \*\*,  $P < 0.01$  (Student  $t$  test). (C) A549 cells were stimulated with 100 ng/ml IFN- $\gamma$  for 24 h or infected with TBEV of the Neudorf strain at an MOI of 0.1, 0.4, or 1. Cells were lysed, separated using SDS-PAGE, blotted, and stained with specific anti-IFITM1 and anti-IFITM3 antibodies.  $\beta$ -Actin was used as a protein loading control.

IFITM3-specific antibody. We detected bands at the expected molecular weight of 14 kDa for all IFITM3 PTM mutants and N-terminal mutants (Fig. 4B). Again, we detected additional lower-mass IFITM3 bands, which were most evident for the Y20A and Y99A mutants, suggesting that these residues might possibly play a role in IFITM3 proteolysis protection or influence the structure of IFITM3 by other means. We could not use the specific IFITM3 monoclonal antibody (MAB), i.e., D8E8G, to detect  $\Delta$ 21N

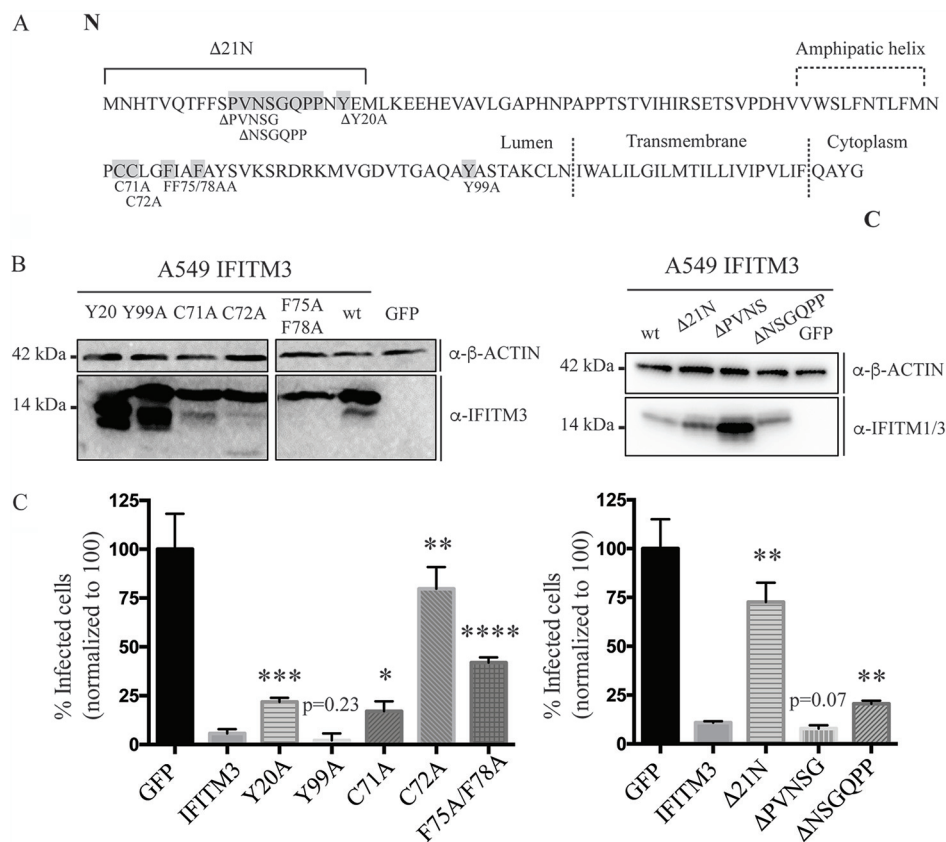


**FIG 4** IFITM3 motifs required for restriction of TBEV infection. (A) Schematic representation of deletions and point mutations introduced into IFITM3. (B) A549 cells stably expressing mutated IFITM3 or an empty cassette were lysed, separated with SDS-PAGE, blotted, and stained with a specific anti-IFITM3 antibody. The blot on the left shows the mutated residues in the FLAG-tagged IFITM3 sequence—Y20, Y299A, C17A, C72A, and F75A/F78A—compared to wild-type FLAG-tagged IFITM3 and the empty vector expressing GFP. The blot on the right shows the N-terminal mutants with deletions—Δ21N, ΔPVNSG, and ΔNSGQPP—compared to the nontagged wild-type IFITM3. β-Actin was used as a protein loading control. (C) A549 cells expressing wild-type and mutated FLAG-tagged IFITM3 were plated in equal quantities and, after 24 h, they were infected with TBEV of the Neudorf strain at an MOI of 0.2. At 24 hpi, the cells were stained with a TBEV E antibody and analyzed by flow cytometry. Values indicate the mean of  $n = 3$  independent experiments  $\pm$  the SD. The statistical significance values ( $P$ ) for each mutant and wild-type IFITM3 are presented. \*,  $P = 0.01$  to  $0.05$ ; \*\*,  $P < 0.01$ ; \*\*\*,  $P < 0.001$ ; \*\*\*\*,  $P < 0.0001$  (Student  $t$  test).

since it recognized an epitope surrounding the V5 residue, which is within the region deleted in the IFITM3 Δ21N mutant. Therefore, we used the MHK2.1 antibody, which recognized an epitope surrounding the EHEV (residues 26 to 29) of both IFITM1 and IFITM3 (43). Even though MHK cross-reacts with IFITM1, endogenous IFITM1 was not detected in the control A549 cells that overexpressed only GFP.

Next, each mutated protein was assessed for its effect on TBEV infection (Fig. 4C). Cells were infected with TBEV at an MOI of 1. At 24 h postinfection (hpi), the cells were fixed, permeabilized, and stained for protein E, and the percentage of E-expressing cells was determined using flow cytometry. The results reveal a significant loss of anti-TBEV activity in cells expressing IFITM3 Δ21N, IFITM3 ΔNSGQPP, IFITM3 Y20A, IFITM3 C72A, and IFITM3 F75A/F78A compared to wild-type IFITM3.

**Spread and cytopathicity of TBEV in A549 IFITM1/2/3 cells.** Next, we sought to analyze the role of IFITM-mediated inhibition of infection on the protection of cells from the cytopathic effect caused by the TBEV infectious cycle. We used a low inoculum of the virus (MOI of 0.01) to infect a high-density cell monolayer for 96 h to gradually observe the cytopathic effect on the cell culture. As shown in Fig. 5A, the expression of IFITM1/2/3 proteins in cells substantially reduced their susceptibility to viral cytopathicity. However, inhibition of the cytopathic effect was lower than expected based on the level of IFITM-mediated infection

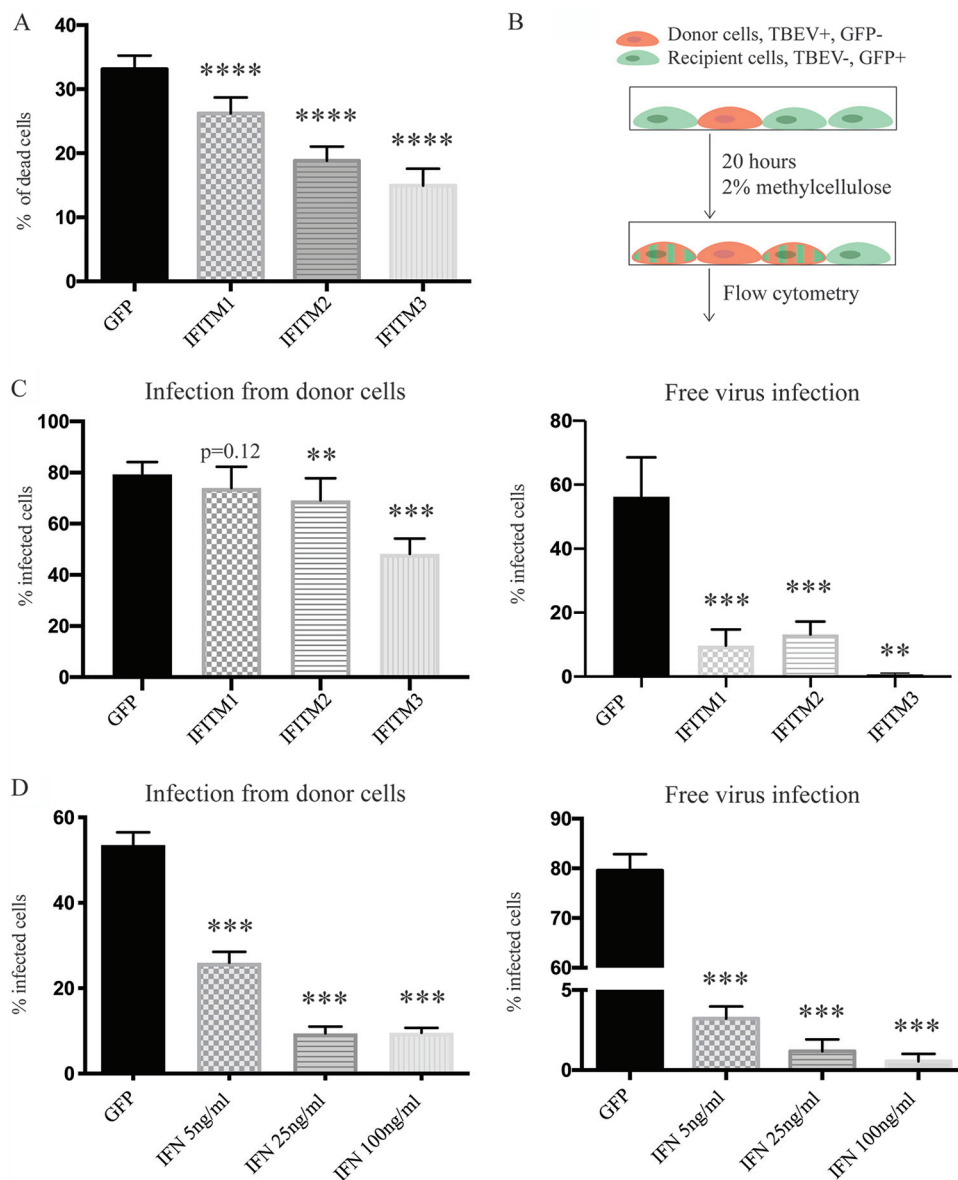


**FIG 5** Cytopathicity and spread of TBEV in A549 IFITM1/2/3 cells. (A) Cytopathic effects of A549 IFITM1/2/3 and control GFP cells resulting from 96 h of TBEV infection at an MOI of 0.1. After staining with trypan blue, the ratio of dead cells to all cells was determined through microscopy. (B) Schematic representation of the coculture assay with limited cell-free infection. A549 donor cells infected with TBEV (red) were cocultured with TBEV-GFP<sup>+</sup> recipient cells (green), covered with semiliquid 2% methylcellulose medium to limit cell-free infection, and cultured for 20 h. The ratio of recipient GFP<sup>+</sup> cells infected by TBEV (stained for TBEV E protein, green/red) to all recipient cells was then determined through flow cytometry. (C) A549 IFITM1/2/3 cells were infected with the cell-free virus at an MOI of 1 or cocultured with TBEV-infected donor cells (wild-type A549 cells). At 24 hpi, the cells were trypsinized, stained for TBEV E protein, and analyzed through flow cytometry. (D) IFN- $\gamma$ -stimulated A549-GFP cells were infected with cell-free virus at an MOI of 1 or cocultured with TBEV-infected donor cells (wild-type A549 cells). At 24 hpi, the cells were trypsinized, stained for TBEV E protein, and analyzed by using flow cytometry.

restriction in previous experiments. For instance, for IFITM3-expressing cells, we obtained only an  $\sim 2$ -fold reduction in the cytopathic effect with respect to the GFP-expressing control line. This suggests that the effect of IFITM-mediated inhibition observed in the widely used 24-h high-MOI assays may not reflect the real protection of cells from TBEV-mediated cell death.

To further characterize the influence of IFITM proteins on the spread of TBEV in the cell monolayer, we decided to analyze IFITM inhibition in the context of potential cell-to-cell transmission of virus. Numerous viruses can efficiently spread through direct cell-to-cell transmission. The ability of viruses to spread without the release of viral particles into extracellular



spaces helps them escape immune responses, especially through avoiding neutralizing antibodies (44). In standard plaque assays performed on high-cell-density monolayers overlaid with a semisolid medium, TBEV was observed to efficiently spread to adjacent cells, creating visible foci that could be stained with anti-E antibody (data not shown). This suggests that TBEV may spread through direct cell-cell contact in monolayers, although it is also possible that there is a limited rate of the spread of the virus through diffusion.

We analyzed the function of the IFITMs in coculture assays, as schematically depicted in Fig. 5B. Wild-type TBEV-infected A549 cells acted as virus donor cells, and uninfected A549 IFITM1/2/3 or A549 GFP cells acted as acceptor cells. All acceptor cell lines stably expressed GFP such that they could be distinguished from wild-type donor cells using flow cytometry. The wild-type cells were infected with TBEV at an MOI of 2. After 2 h, the cells were washed with a low-pH buffer to inactivate cell-bound virus particles, trypsinized, and seeded with acceptor cells at a ratio of 1:4. After 2 h, the attached cells were overlaid with a semiliquid medium containing methylcellulose to limit the spread of cell-free virions and were incubated for another 20 h to allow for production and spread of the virus to neighboring cells. To measure the level of TBEV infection of the GFP-expressing acceptor cells, we employed a gating strategy in which cells that expressed high levels of GFP were analyzed for production of the TBEV E antigen. As shown in Fig. 5C, the IFITM proteins efficiently inhibited TBEV transmission when cell-free infection was allowed. After infection at an MOI of 1 for 24 h, 64% of the A549-GFP control cells were infected compared to 14% of the A549-IFITM1 cells, 17% of the A549-IFITM2 cells, and only 1% of the A549-IFITM3 cells. The level of inhibition of cell-free infection by IFITM was in accordance with the results obtained through virus titration (Fig. 2A) and immunofluorescence (Fig. 2C), where dramatic inhibition of TBEV by IFITM3 was also observed. However, in the methylcellulose-overlay assay, where the infected donor cells were used as the “inoculum” and viral diffusion was limited, the IFITMs inhibited infection to a much lower extent (Fig. 5C). The reduced infection rate in cocultures was not statistically significant for the A549-IFITM1 cells and was only moderately significant for the A549-IFITM2 and A549-IFITM3 cells. The results show differences in IFITM-dependent TBEV infection modulation between the two viral entry modes: when free virus particles suspended in a cell medium are delivered as an inoculum and when virus-infected donor cells serve as the source of infectious viral particles. This suggests that IFITM proteins could inhibit the entry of the virus less efficiently if the virus enters directly from adjacent cells.

Since IFITM-mediated viral restriction is a part of the IFN-induced antiviral response, it was interesting to analyze how IFN inhibited viral infection when viral diffusion was limited. We performed a similar coculture assay with TBEV-infected wild-type donor A549 cells and acceptor A549-GFP cells stimulated with IFN- $\gamma$  and compared the results to those of the free-infection assays (Fig. 5D). Again, IFN- $\gamma$  potently inhibited TBEV infection with the cell-free virus inoculum at all tested concentrations. However, when the A549-GFP cells were cocultured with infected donor cells and overlaid with methylcellulose, inhibition by IFN- $\gamma$  was notably less efficient.

These results emphasize the challenge of understanding how viruses actually spread in tissues in living organisms. In fact, in commonly used *in vitro* assays, a viral inoculum is added to cells and, after some time, viral infection is detected using different methods. However, our results suggest that the virus spreads to neighboring cells without entering the extracellular space and may thus be less prone to IFITM-mediated inhibition.

## DISCUSSION

As major effectors of IFN signaling, IFITM proteins have been shown to inhibit the replication of different flaviviruses, including dengue virus, West Nile virus, and Zika virus (45, 46). However, no studies regarding the role of IFITMs in the infection of TBEV, an important pathogen of humans, have been published. The type I IFN response was demonstrated to be critical for the protection of mice against TBEV (31) and other insect-borne flavivirus infections, including Zika virus (30), and these findings show that tick-borne flaviviruses are able to antagonize IFN signaling, resulting in their evasion from host innate immunity (33). Here, we aimed to analyze the role of IFITM proteins in TBEV infection and *in vitro* transmission of TBEV.

First, we tested whether IFN modulates TBEV infection in A549 cells, which are commonly used for RNA virus infections. We found that stimulation of A549 with IFN- $\gamma$  led to a dramatic reduction in the TBEV titer, confirming the role of IFN signaling in TBEV infection (Fig. 1A). In order to investigate the role of the antiviral IFITM1, IFITM2, and IFITM3 proteins in TBEV infection, we generated polyclonal A549 cell lines that stably expressed N-terminally tagged IFITM proteins together with GFP protein, which was independently translated due to the insertion of an IRES sequence (Fig. 1B). We detected similar levels of expression of the IFITM1/2/3 proteins in the generated cell lines (Fig. 1C and D), whereas in wild-type A549 cells stimulated with IFN- $\gamma$ , we detected only modest expression of IFITM1 and IFITM3. We then analyzed the influence of the overexpressed IFITM proteins on TBEV infection *in vitro*. Through several different approaches, we demonstrated the effective inhibition of TBEV infection by all IFITM (IFITM1/2/3) proteins (Fig. 2). The IFITM1 protein is mainly localized at the plasma membrane and at endosomal membranes, whereas IFITM2 and IFITM3 reside in endosomal and lysosomal membranes (36). Therefore, IFITM1 effectively prevents the fusion of viruses that enter through plasma membranes and in early endosomes, whereas IFITM2, as well as IFITM3, acts more strongly against viruses that enter cells through the late endosomal pathway (46). In keeping with observations for other flaviviruses (45), we showed that TBEV was most potently restricted by IFITM3, leading to a dramatic decrease in the TBEV protein E level and the titers of both intracellular and secreted TBEV (Fig. 2A). This is consistent with the fact that flaviviruses enter the cells through receptor-mediated endocytosis, followed by the acidification-induced fusion of the viral envelope and endosomal membranes (47).

To analyze the role of endogenous cellular IFITMs, we developed IFITM knockout cell lines. Several previous reports analyzed viral infection levels in cells with IFITMs that were downregulated by siRNA. Because siRNA, *per se*, induces IFN signaling in cells (48), we decided to implement CRISPR-Cas9 to investigate mutant cell lines in a non-IFN-stimulated context. Since the A549 cells expressed detectable levels of IFITM1 and IFITM3, we generated single knockouts (IFITM1-KO and IFITM3-KO) and a double knockout (IFITM1/3-KO). The knockout status of all generated cell lines was validated by Western blotting (Fig. 3A). CRISPR-Cas9 has previously been implemented to investigate the role of IFITMs in viral infection (49), but single IFITM1 and IFITM3 knockout mutants, as well as the double IFITM1/IFITM3 knockout mutants, have not been previously described. As expected, cell clones that expressed undetectable or very small amounts of IFITM1 or IFITM2 were significantly more susceptible to viral infection. Moreover, the double IFITM1/3 knockout conferred the highest susceptibility to infection—a >8-fold increase with respect to wild-type A549 cells—which confirmed the results of other reports on the additive effects of IFITM proteins in viral infection (49). Since the cells were not stimulated with IFN before TBEV infection in this assay, the results of inhibition demonstrate the potency of the IFITMs produced in A549 cells at basal levels or induced through TBEV sensing soon after infection. Collectively, the results of the overexpression and knockout experiments demonstrate the major role of IFITM proteins in suppressing TBEV infection in standard *in vitro* infection assays, with IFITM3 having the most potent effect.

Several structural motifs and posttranslational modifications are implicated in IFITM3-mediated antiviral resistance mechanisms (38). To broaden the understanding of IFITM3-mediated TBEV inhibition, we set out to identify IFITM3 motifs that are important for the modulation of TBEV infection. We employed a mutagenesis analysis to investigate the roles of palmitoylation, phosphorylation, and oligomerization motifs, as well as the N-terminal domain of IFITM3 in its antiviral function against TBEV. We showed that mutation of the S-palmitoylation site at residue C72, those at the oligomerization site at residues F75 and F78, and the deletions in the 21-aa N-terminal domain significantly compromised the antiviral activity of IFITM3 against TBEV. This is in accordance with earlier data on the roles of these motifs in the entry of IAV and the dengue virus, both of which enter cells through pH-dependent endocytosis (38, 39, 41, 50). In contrast, deletion of the IFITM3 N-terminal domain did not compromise the suppression of HIV-1, whose entry is pH independent (41), and enhanced the suppression of HCV (36). We also tested small deletions in the N-terminal domain and found that they either did not impact the antiviral role of IFITM3 ( $\Delta$ PNVSG) or did significantly impact it, but to a lesser

extent ( $\Delta$ NSGQPP). In addition, the anti-TBEV activity of IFITM3 was partially suppressed by mutations in the Y20 N-terminal phosphorylation site, suggesting that different motifs in the 21-aa N-terminal domain may coordinate to confer the anti-TBEV functions of IFITM3. We did not detect any losses of activity in IFITM3 when mutated at the Y99 phosphorylation site. Similarly, Y99A mutation did not lead to a loss of protection against the dengue virus, while it led to a loss of function against IAV (39) and revealed a mixed phenotype for coronavirus infection (40).

Having confirmed the role of IFITM proteins in TBEV infection through the quantitative analysis of infected cells, we aimed to investigate IFITM-mediated protection against TBEV-induced cell death. We used a low MOI to infect a high-density cell monolayer to gradually analyze the cytopathic effect in cell cultures. Surprisingly, the protective effect of the IFITM proteins was weaker than expected (Fig. 5A). For example, even though IFITM3 overexpression led to an  $\sim$ 10-fold decrease in the number of infected cells in a 24-h infection cycle, it led only to an  $\sim$ 2-fold decrease in the number of cell deaths over 96 h. We hypothesized that the direct spread of TBEV between cells in a high-density monolayer could be more resistant to the protective action of IFITM than through cell-free entry. In fact, most studies reporting the antiviral effects of IFITMs are based on single-round free viral infection experiments on IFITM-overexpressing cells.

Certain viruses are able to infect neighboring cells without leaving the extracellular space. This enables them to escape neutralizing antibodies and other components of the host immune responses. Cell-to-cell spread is well described for some viruses, including herpesviruses, orthomyxoviruses, poxviruses, and rhabdoviruses. For other viruses, such as HCV (a virus belonging to the *Flaviviridae* family), the importance of this phenomenon in viral pathogenesis is not as well understood (44). In IFITM-expressing hepatic cells, the viral foci of HCV were smaller, suggesting a possible inhibitory effect of IFITM proteins on this route of infection; however, no quantitative analyses were performed (21). Little is known about cell-to-cell transmission of flaviviruses. In a recent study, the neurotropic Japanese encephalitis virus was found to be able to spread from human microglia to neighboring cells in a contact-dependent cell-to-cell manner (51). In another report, dengue virus infected neighboring mosquito cells through direct cell-to-cell transmission, which required tetraspanin C189 (52). To our knowledge, there have been no studies investigating cell-to-cell TBEV transmission. TBEV formed infection foci in a high-density A549 cell culture when free diffusion was suppressed in a viscous medium, which is one of the indicators that there is cell-to-cell spread. In addition, the infection rate in cocultures overlaid with a semiliquid medium was as high as in nonoverlaid cultures (data not shown). However, more experimental evidence is needed in order to understand the role of the cell-to-cell spread of TBEV in its pathogenesis, preferably evidence from neuronal cells or *in vivo*. A widely used approach to examining cell-to-cell spread is the use of neutralizing antibodies that block cell-free viruses. However, some cell-cell contacts may remain sensitive to antibody-mediated neutralization (53). Cell-to-cell HCV spread was reported to be limited by an anti-HCV nanobody and sera from vaccinated animals (54, 55). Therefore, investigation of cell-to-cell spread is challenging, and it is necessary to combine different experimental functional and imaging approaches.

Viral transmission across tight cell-cell contacts allows viruses to evade immune responses. Here, we showed that TBEV transmission in cocultures was less prone to IFITM-mediated inhibition than infection with a cell-free inoculum. Since IFITMs are effectors of intrinsic IFN-induced antiviral responses, we next investigated the influence of IFN stimulation on infection, which was carried out with a cell-free virus and infected donor cells. We showed that IFN- $\gamma$  protected cells to a much lesser extent when the acceptor cells were incubated with infected donor cells than during cell-free infection. Similar findings were reported for HIV-1; cell-to-cell transmission allowed the virus to bypass IFITM restriction in target cells. However, IFITMs limited the spread of HIV-1 from infectious cells by rendering virions less infectious (27, 29). Thus, our findings are in agreement with those of HIV studies and suggest that overcoming IFITM restriction through cell-to-cell spread might be a more universal phenomenon. In addition, cell-to-cell transmission of HIV-1 was less sensitive to IFN, since higher concentrations of IFN were required to suppress direct cell-to-cell transfer

than for cell-free infection (56). Moreover, the antiviral actions of other IFN-induced proteins—namely, TRIM5 $\alpha$  and tetherin—were less effective against the cell-to-cell spread of retroviruses through virological synapses than against cell-free infection (57–59). Direct cell transmission was also able to the lower effectiveness of antiviral strategies against HIV-1 (60), HCV (61), and influenza (62).

We propose two possible explanations for the suboptimal activity of IFITMs in coculture assays. First, the mechanism of TBEV entry from adjacent cells may differ from the mechanism of cell-free entry, and it may be less prone to inhibition by IFITM. Second, the direct cell-to-cell transmission of the virus may involve the retention of the virus at the surface of producer cells, thus increasing the local density of viral particles. The high local MOIs reached at sites of cell-cell contact may result in more efficient transmission and may overcome some saturable cellular barriers. More studies are needed—optimally, *in vivo*—to better understand the roles of IFN and particular ISGs in direct viral spread. The ability to block cell-to-cell spread would be an important aspect of any antiviral approach to TBEV infection.

In summary, we demonstrated here the important role of IFITM proteins in the inhibition of TBEV infection, with the most significant role being that of the IFITM3 protein, including the dissection of its functional motifs. However, our data suggest that TBEV may partially escape IFN- and IFITM-mediated suppression during infection in high-density cultures, as the viruses can pass directly from donor cells to naive recipient cells. Cell-to-cell spread may constitute a strategy for escape from host innate defenses.

## MATERIALS AND METHODS

**Cells and viruses.** A549 cells (ATCC CCL-185) were cultured in Dulbecco modified Eagle medium (DMEM; with 4.5 g/liter glucose and L-glutamine) (Corning), supplemented with 10% fetal bovine serum (FBS) and 1% penicillin-streptomycin, and incubated at 37°C with 5% CO<sub>2</sub>. GP2-293 packaging cells (Clontech) were cultured in IMDM (with L-glutamine and 25 mM HEPES; Lonza Bioscience), supplemented with 10% FBS and 1% antibiotic-antimycotic solution (Gibco), and incubated at 37°C with 5% CO<sub>2</sub>. TBEV virus, Neudorf strain, was kindly provided by Karin Stiasny (Center for Virology, Medical University of Vienna, Vienna, Austria). The virus was grown in A549 cells, and titers were determined using a plaque assay.

**Generation of stable A549 cell lines producing IFITM variants.** Expression plasmids of the IFITM family were obtained from Addgene (HA-hIFITM1, plasmid 58399; HA-hIFITM2, plasmid 58398; and Myc-hIFITM3, plasmid 58461). To obtain cells that expressed N-terminally FLAG-tagged IFITM1/2/3 proteins, the cDNA sequences of IFITM1, IFITM2, and IFITM3 were amplified using PCR with the forward primers carrying the BamHI restriction site and FLAG tag sequence and reverse primers carrying the EcoRI restriction site (IFITM1, forward [AATTGGATCCACCATGGACTACAAGGACGATGACGATAAACACAAGGAGGAACATGAGGT] and reverse [AATTGAATTCCTAGTAACCCGCTTTTCTCTG]; IFITM2, forward [AATTGGATCCACCATGGACTACAAGGACGATGACGATAAAACACATTGTGCAACCTTCT] and reverse [AATTGAATTCCTATCGCTGGGCTGGACGAC]; IFITM3, forward [AATTGGA TCCACCATGGACTACAAGGACGATGACGATAAAATCACA CTGTCCTCAACCTTCT] and reverse [AATTGAATTCCTATC CATAGGCTGGGAAGA]). The amplified sequences were cloned into a pJET plasmid (SnapGene) and validated with Sanger sequencing. Y20A, Y99A, C71A, C72A, and F75AF78A mutations were introduced into pJET-FLAG-IFITM3 through site-directed mutagenesis using the Quick-Change Lightning site-directed mutagenesis kit (Agilent) and primers designed for mutagenesis (Y20A, forward [GTGGCCAGCCCCCAACGCCGAGATGCTCAA GGAG] and reverse [CTCCTTGAGCATCTCGGCTGGGGGGCTGGCCAC]; Y99A, forward [GGGGCCAGGCCGCCG CTCCACCGCCAAG] and reverse [CTTGGCGGTGGAGGCGGCGCTGGGCCCC]; C71A, forward [CTTCATGAACCCCG CCTGCCTGGGCTTCATAGC] and reverse [GCTATGAAGCCAGGCAGGCGGGGTTTCATGAAG]; C72A, forward [CTTC ATGAACCCCTGCGCCCTGGGCTTCATAGC], reverse [GCTATGAAGCCAGGCGCAGGGGTTTCATGAAG]; F75AF78A, forward [CCTGTGCTGGCGCCATAGCAGCCGCTACTCCGTGAAG] and reverse [CTTCACGAGTAGGCGGCTGCT ATGGCGCCAGGCAGCAGG]). Sequences coding for IFITM3 without a FLAG tag (no tag) and for IFITM3 with an N-terminal deletion of 21 aa ( $\Delta$ 21N) were generated through PCR using specifically designed primers (no-tag, forward [TATGGATCCACCATGAATCACACTGTCCAAACCTTC] and reverse [AATTGAATTCCTATCCATAGGCTGGAA GA]; and  $\Delta$ 21N, forward [TAGGATCCACCATGCTCAAGGAGGAGCAGAG] and reverse [AATTGAATTCCTATCCATA GGCCTGGAAGA]). The  $\Delta$ PNVNSG and  $\Delta$ NSGQPP mutants were constructed using the pJET-IFITM3-no-tag as the template and a Quick-Change Lightning site-directed mutagenesis kit (Agilent) ( $\Delta$ PNVNSG, forward [CTGTCCA AACCTTCTCTCAGCCCCCAACTATGAGATG] and reverse [CATCTCATAGTTGGGGGGCTGAGAGAAGAAGGTTTG GACAG];  $\Delta$ NSGQPP, forward [CAAACCTTCTCTCTCTGCACTATGAGATGCTCAAGG] and reverse [CCTTGAGCAT CTCATAGTTGACAGGAGAGAGAAGGTTTG]). All IFITM1/2/3 variants were cloned into the pLZRS-IRES-GFP retrovirus vector using the BamHI and EcoRI sites. The Phoenix Amphi packaging system was used to obtain recombinant retroviral vectors as previously described (63). Briefly, pLZRS-IRES-GFP carrying the IFITM1/2/3 sequences were transfected, together with a pVSV-G plasmid, into GP2-293 cells. For retrovirus carrying solely GFP, pLZRS-IRES-GFP empty plasmid and pVSV-G were transfected into GP2-293 cells. After 48 h, retrovirus-containing supernatants were collected from the GP2-293 cells, centrifuged, filtered, and used for the transduction of A549 cells. Using a FACSCalibur flow cytometer sorting option (Becton Dickinson), GFP-positive cells were sorted to obtain cell lines that were at least 95% positive.

**Generation of A549-IFITM1/3-KO monoclonal cell lines.** A panel of monoclonal A549 cell lines with single knockouts (A549-IFITM1-KO and A549-IFITM3-KO) and with a double knockout (A549-IFITM1/IFITM3-KO) was generated. To generate these knockouts, single guide RNA (sgRNA) sequences (for IFITM1, forward [TCCAAGGTCCACCGTGATCA]; for IFITM3, forward [GTCAACAGTGGCCAGCCCC]) were cloned into the lentiCRISPRv2 expression vector (64). These sequences were designed to target the N termini of IFITM1 and IFITM3, respectively. The wild-type A549 cells were transduced with the lentivirus vector containing the IFITM1 or IFITM3 sgRNA sequence or both vectors. The following day, the medium with the lentivirus was removed and replaced with fresh media containing 10  $\mu$ g/ml puromycin. Selection pressure with puromycin was continued for up to 72 h, and the cells were then sorted as single cells into a 96-well plate using fluorescence-activated cell sorting. Next, the cells were propagated to form colonies that had originated from a single cell. Individual clones were screened using Western blotting to identify clones with reduced or nondetectable IFITM1 and/or IFITM3 protein expression.

**Protein expression analysis.** For detection of intracellular TBEV E protein, the A549 cells plated in 2.5-cm culture dishes in complete DMEM were infected with TBEV at an MOI of 1 for 24 h. For detection of IFITM proteins, A549 cells that stably expressed IFITMs or wild-type A549 cells were plated in 12-well culture dishes. For IFN stimulation, IFN- $\gamma$  recombinant human protein (Gibco) was added to cells at 100 ng/ml for 24 h. The cells were washed with PBS and lysed in a buffer containing 150 mM NaCl, 1% Tergitol-type NP-40, 50 mM Tris (pH 8), 50 mM NaF, 5 mM EDTA, and a protease inhibitor cocktail (Bimake.com). Proteins were separated using 10% SDS-PAGE and blotted onto a polyvinylidene difluoride membrane. To detect TBEV E protein, nonreducing conditions were used. The membranes were blocked with 5% milk in PBS with 0.05% Tween 20 and probed with the following antibodies: anti-flavivirus E (clone D1-4G2-4-15 [4G2], 1:1,000; Absolute Antibody) anti-IFITM1 (clone 60074-I-Ig, 1:1,000; Proteintech), anti-IFITM2 (clone 66137-I-Ig, 1:1,000; Proteintech), anti-IFITM3 (clone D8E8G, 1:1,000; Cell Signaling), anti-IFITM1/3 MHK2.1 (a monoclonal antibody recognizing an epitope surrounding the EHEV [residues 26 to 29] of both IFITM1 and IFITM3; 1:2,000) (43), and anti-FLAG M2 MAb (1:1,000; Sigma). Mouse anti-human  $\beta$ -actin (1:5,000; Novus Biologicals) was used as a loading control. After incubation with goat anti-mouse or goat anti-rabbit horseradish peroxidase-conjugated secondary antibodies (1:2,000; Santa Cruz Biotechnology), the membranes were developed using enhanced chemiluminescence (ECL). For detection of the TBEV E protein in the A549 cell medium, proteins were precipitated by shaking with 10% trichloroacetic acid at 4°C overnight, centrifuged for 20 min at 13,000 rpm at 4°C, washed two times with ice-cold 80% acetone, and resuspended in PBS. The protein concentration was determined by using a Quick-Start Bradford protein assay kit (Bio-Rad). For immunoprecipitation of IFITM1, A549 cells were stimulated with 100 ng/ml IFN- $\gamma$  for 24 h, harvested into 1% NP-40 lysis buffer, and lysed for 20 min on ice. After centrifugation at 14,000 rpm at 4°C for 30 min, the cell lysate was mixed with 2  $\mu$ l of CVY rabbit serum (Moravian Biotechnologies) generated against the C terminus of IFITM1, followed by incubation overnight at 4°C. Protein G-agarose beads (Thermo Fisher) were used to pull down the antibody-protein complex. Proteins were eluted in 1 $\times$ LDS buffer (NuPAGE; Thermo Fisher) with 0.1 M dithiothreitol at 95°C for 10 min and then subjected to SDS-PAGE.

**Immunofluorescence.** A549 cells were grown on a microcover glass, fixed with 4% paraformaldehyde in phosphate-buffered saline (PBS), permeabilized with 0.2% Triton X-100 in PBS for 5 min, and washed three times with PBS. FLAG-tagged IFITM1/2/3 proteins were stained with anti-FLAG MAb (1:2,000; Sigma), and TBEV protein E was stained with anti-flavivirus E Ig, clone D1-4G2-4-15 (4G2, 1:500; Absolute Antibody). Antibody dilutions were prepared in PBS with 1% bovine serum albumin (Sigma). After three washes with PBS, the cells were incubated with Alexa 546-conjugated goat anti-mouse secondary antibodies (1:3,000; Molecular Probes). After three washes with PBS, the cells were treated with ProLong Diamond Antifade Mountant with (4',6'-diamidino-2-phenylindole; Invitrogen) to visualize the nuclei. The images were analyzed using a Nikon ECLIPSE TE300 confocal laser-scanning microscope.

**Flow cytometry.** A549 cells were stained for the intracellular expression of TBEV protein E using indirect immunofluorescence. Infected and mock-infected cells were trypsinized, washed with PBS, and then fixed and permeabilized using a Cytofix/Cytoperm fixation/permeabilization solution kit (BD Biosciences). The cells were stained with mouse monoclonal antibodies for anti-flavivirus E (1:300; Absolute Antibody) in PermWash buffer (BD Biosciences) and, as a second step, goat anti-mouse Ig-phycoerythrin (BD Biosciences). Labeled cells were analyzed with a Guava easyCyte flow cytometer (Luminex).

**TBEV titration.** Monolayers of A549 cells were cultured in 24-well plates and inoculated with 10-fold dilutions of TBEV for 2 h. After the removal of the virus, the cells were washed with PBS and overlaid with 1% carboxymethyl cellulose in DMEM. After 5 days, the medium was removed, and the cells were washed with PBS three times. The monolayers were stained with naphthalene black to visualize plaques. Virus titers are expressed as PFU/ml.

**Cell viability assay.** A549 IFITM1/2/3 or control GFP cells were infected with TBEV of the Neudorf strain at an MOI of 0.1 PFU/cell. After 96 h, when the cytopathic effect was clearly visible, the medium with cells was collected, and the adhering cells were trypsinized and pooled with the rest of the medium. The cells were then stained with trypan blue, and the ratio of dead cells was determined using light microscopy by counting at least 500 cells.

**Cell coculture assay.** Wild-type A549 cells were infected with TBEV of the Neudorf strain at an MOI of 3 PFU/cell. These cells were then used as TBEV donor cells while being used as acceptor cells. The latter cells stably express GFP translated from the IRES of the IFITM1/2/3-encoding cassette. At 2 hpi, the donor cells were washed with low-pH citrate buffer (135 mM NaCl, 10 mM KCl, 40 mM citric acid [pH 3.0]) to inactivate cell-bound viral particles, trypsinized, and counted. A 1:4 ratio of donor to acceptor cells was used, and a total of  $2 \times 10^5$  cells were seeded in 24-well plates in triplicate. After 2 h, the cell medium was removed, and the attached cells were covered with fresh semiliquid medium containing



2% methylcellulose and cultured an additional 20 h. Finally, the cells were trypsinized, fixed, stained for TBEV E protein, and analyzed with flow cytometry for the E protein and GFP expression.

**Statistical analysis.** Since the populations were normally distributed, an unpaired two-tailed *t* test was used to determine whether there were significant differences. Statistically significant differences are indicated in the figures by asterisks (\*,  $P = 0.01$  to  $0.05$ ; \*\*,  $P < 0.01$ ; \*\*\*,  $P < 0.001$ ; \*\*\*\*,  $P < 0.0001$ ). Unless stated otherwise, the data are representative of three independent experiments.

## ACKNOWLEDGMENTS

We thank Karin Stiasny from the Center for Virology, Medical University of Vienna, Vienna, Austria, for the TBEV Neudorf strain.

A.M.C. acquired funding and administered the project. A.M.C., M.G.-H., P.G., M.N., M.T., A.D.L., M.R., and W.H. performed the experiments. E.K., M.N., B.V., and R.D.S. provided reagents. A.M.C. and M.G.-H. wrote the original draft. A.M.C., B.V., K.B.-S., T.H., and K.B. supervised group members. A.D.L., R.D.S., K.B.-S., T.H., and K.B. edited the article. All authors read and approved the final manuscript.

This research was funded by POWROTY/Reintegration program of the Foundation for Polish Science cofinanced by the European Union under the European Regional Development Fund (project POIR.04.04.00-00-3E52/17-00) and The International Centre for Cancer Vaccine Science, a project carried out within the International Research Agendas program of the Foundation for Polish Science cofinanced by the European Union under the European Regional Development Fund (project MAB/2017/3). B.V. was funded by the European Regional Development Fund (Project ENOCH, No.CZ.02.1.01/0.0/0.0/16\_019/0000868); by the Ministry of Health, Czech Republic; and by MMCI, a conceptual development of research organization (grant 00209805). M.N. was funded by The Grant Agency of the Czech Republic (grant 18-23773Y). The Neudorf TBEV strain propagation was funded by the National Science Centre, Poland, under grant UMO-2015/19/D/NZ6/01717 (PI E.K.).

B.V. is associated with Moravian Biotechnology, the company that developed the CYV polyclonal sera, as a consultant. The company did not provide financial support for these studies and had no influence on the design, execution, or analysis of the experiments. We declare there are no conflicts of interest.

## REFERENCES

- Bogovic P, Strle F. 2015. Tick-borne encephalitis: a review of epidemiology, clinical characteristics, and management. *World J Clin Cases* 3:430–441. <https://doi.org/10.12998/wjcc.v3.i5.430>.
- Donoso Mantke O, Escadafal C, Niedrig M, Pfeffer M, on behalf of The Working Group for Tick-Borne Encephalitis. 2011. Tick-borne encephalitis in Europe, 2007 to 2009. *Euro Surveill* 16:19976. <https://doi.org/10.2807/ese.16.39.19976-en>.
- Alfano N, Tagliapietra V, Rosso F, Ziegler U, Arnoldi D, Rizzoli A. 2020. Tick-borne encephalitis foci in northeast Italy revealed by combined virus detection in ticks, serosurvey on goats and human cases. *Emerg Microbes Infect* 9:474–484. <https://doi.org/10.1080/22221751.2020.1730246>.
- Boelke M, Bestehorn M, Marchwald B, Kubinski M, Liebig K, Glanz J, Schulz C, Dobler G, Monazahian M, Becker SC. 2019. First isolation and phylogenetic analyses of tick-borne encephalitis virus in Lower Saxony, Germany. *Viruses* 11:462. <https://doi.org/10.3390/v11050462>.
- Gould EA, Solomon T. 2008. Pathogenic flaviviruses. *Lancet* 371:500–509. [https://doi.org/10.1016/S0140-6736\(08\)60238-X](https://doi.org/10.1016/S0140-6736(08)60238-X).
- Gritsun TS, Lashkevich VA, Gould EA. 2003. Tick-borne encephalitis. *Antiviral Res* 57:129–146. [https://doi.org/10.1016/S0166-3542\(02\)00206-1](https://doi.org/10.1016/S0166-3542(02)00206-1).
- Andersson CR, Vene S, Insulander M, Lindquist L, Lundkvist A, Günther G. 2010. Vaccine failures after active immunization against tick-borne encephalitis. *Vaccine* 28:2827–2831. <https://doi.org/10.1016/j.vaccine.2010.02.001>.
- Morozova OV, Bakhvalova VN, Potapova OF, Grisechkin AE, Isaeva EI, Aldarov KV, Klinov DV, Vorovich MF. 2014. Evaluation of immune response and protective effect of four vaccines against the tick-borne encephalitis virus. *Vaccine* 32:3101–3106. <https://doi.org/10.1016/j.vaccine.2014.02.046>.
- Petry M, Palus M, Leitzen E, Mitterreiter JG, Huang B, Kröger A, Verjans GMGM, Baumgärtner W, Rimmelzwaan GF, Růžek D, Osterhaus A, Prajeeth CK. 2021. Immunity to TBEV related flaviviruses with reduced pathogenicity protects mice from disease but not from TBEV entry into the CNS. *Vaccines* 9:196. <https://doi.org/10.3390/vaccines9030196>.
- Zhang Y, Zhang W, Ogata S, Clements D, Strauss JH, Baker TS, Kuhn RJ, Rossmann MG. 2004. Conformational changes of the flavivirus E glycoprotein. *Structure* 12:1607–1618. <https://doi.org/10.1016/j.str.2004.06.019>.
- Li L, Lok S-M, Yu I-M, Zhang Y, Kuhn RJ, Chen J, Rossmann MG. 2008. The flavivirus precursor membrane-envelope protein complex: structure and maturation. *Science* 319:1830–1834. <https://doi.org/10.1126/science.1153263>.
- Pulkkinen LIA, Butcher SJ, Anastasina M. 2018. Tick-borne encephalitis virus: a structural view. *Viruses* 10:350–320. <https://doi.org/10.3390/v10070350>.
- Goto A, Yoshii K, Obara M, Ueki T, Mizutani T, Kariwa H, Takashima I. 2005. Role of the N-linked glycans of the prM and E envelope proteins in tick-borne encephalitis virus particle secretion. *Vaccine* 23:3043–3052. <https://doi.org/10.1016/j.vaccine.2004.11.068>.
- Perera-Lecoin M, Meertens L, Carnec X, Amara A. 2013. Flavivirus entry receptors: an update. *Viruses* 6:69–88. <https://doi.org/10.3390/v6010069>.
- Acosta EG, Castilla V, Damonte EB. 2009. Alternative infectious entry pathways for dengue virus serotypes into mammalian cells. *Cell Microbiol* 11: 1533–1549. <https://doi.org/10.1111/j.1462-5822.2009.01345.x>.
- Kroschewski H, Allison SL, Heinz FX, Mandl CW. 2003. Role of heparan sulfate for attachment and entry of tick-borne encephalitis virus. *Virology* 308:92–100. [https://doi.org/10.1016/S0042-6822\(02\)00097-1](https://doi.org/10.1016/S0042-6822(02)00097-1).
- Protopopova EV, Sorokin AV, Kononova SN, Kachko AV, Netesov SV, Loktev VB. 1999. Human laminin binding protein as a cell receptor for the tick-borne encephalitis virus. *Zentralblatt Für Bakteriologie* 289:632–638. [https://doi.org/10.1016/S0934-8840\(99\)80021-8](https://doi.org/10.1016/S0934-8840(99)80021-8).
- Bluyssen HA, Muzaffar R, Vlietstra RJ, van der Made AC, Leung S, Stark GR, Kerr IM, Trapman J, Levy DE. 1995. Combinatorial association and abundance of components of interferon-stimulated gene factor 3 dictate the selectivity of interferon responses. *Proc Natl Acad Sci U S A* 92:5645–5649. <https://doi.org/10.1073/pnas.92.12.5645>.
- Muller M, Laxton C, Briscoe J, Schindler C, Improta T, Darnell JE, Jr, Stark GR, Kerr IM. 1993. Complementation of a mutant cell line: central role of the

- 91-kDa polypeptide of ISGF3 in the interferon- $\alpha$  and - $\gamma$  signal transduction pathways. *EMBO J* 14:221–228.
20. Huang I-C, Bailey CC, Weyer JL, Radoshitzky SR, Becker MM, Chiang JJ, Brass AL, Ahmed AA, Chi X, Dong L, Longobardi LE, Boltz D, Kuhn JH, Elledge SJ, Bavari S, Denison MR, Choe H, Farzan M. 2011. Distinct patterns of IFITM-mediated restriction of filoviruses, SARS coronavirus, and influenza A virus. *PLoS Pathog* 7:e1001258. <https://doi.org/10.1371/journal.ppat.1001258>.
  21. Wilkins C, Woodward J, Lau DT-Y, Barnes A, Joyce M, McFarlane N, McKeating JA, Tyrrell DL, Gale M. 2013. IFITM1 is a tight junction protein that inhibits hepatitis C virus entry. *Hepatology* 57:461–469. <https://doi.org/10.1002/hep.26066>.
  22. Bailey CC, Zhong G, Huang I-C, Farzan M. 2014. IFITM-family proteins: the cell's first line of antiviral defense. *Annu Rev Virol* 1:261–283. <https://doi.org/10.1146/annurev-virology-031413-085537>.
  23. Jiang D, Weidner JM, Qing M, Pan X-B, Guo H, Xu C, Zhang X, Birk A, Chang J, Shi P-Y, Block TM, Guo J-T. 2010. Identification of five interferon-induced cellular proteins that inhibit West Nile virus and dengue virus infections. *J Virol* 84:8332–8341. <https://doi.org/10.1128/JVI.02199-09>.
  24. Miyauchi K, Kim Y, Latinovic O, Morozov V, Melikyan GB. 2009. HIV enters cells via endocytosis and dynamin-dependent fusion with endosomes. *Cell* 137:433–444. <https://doi.org/10.1016/j.cell.2009.02.046>.
  25. Lu J, Pan Q, Rong L, He W, Liu S-L, Liang C. 2011. The IFITM proteins inhibit HIV-1 infection. *J Virol* 85:2126–2137. <https://doi.org/10.1128/JVI.01531-10>.
  26. Jia R, Ding S, Pan Q, Liu S-L, Qiao W, Liang C. 2015. The C-terminal sequence of IFITM1 regulates its anti-HIV-1 activity. *PLoS One* 10:e0118794. <https://doi.org/10.1371/journal.pone.0118794>.
  27. Tartour K, Nguyen X-N, Appourchaux R, Assil S, Barateau V, Bloyet L-M, Burlaud Gaillard J, Confort M-P, Escudero-Perez B, Gruffat H, Hong SS, Moroso M, Reynard O, Reynard S, Decembre E, Ftaich N, Rossi A, Wu N, Arnaud F, Baize S, Dreux M, Gerlier D, Paranhos-Baccala G, Volchkov V, Roingard P, Cimarelli A. 2017. Interference with the production of infectious viral particles and bimodal inhibition of replication are broadly conserved antiviral properties of IFITMs. *PLoS Pathog* 13:e1006610. <https://doi.org/10.1371/journal.ppat.1006610>.
  28. Lee W-YJ, Fu RM, Liang C, Sloan RD. 2018. IFITM proteins inhibit HIV-1 protein synthesis. *Sci Rep* 8:1–15.
  29. Compton AA, Bruel T, Porrot F, Mallet A, Sachse M, Euvrard M, Liang C, Casartelli N, Schwartz O. 2014. IFITM proteins incorporated into HIV-1 virions impair viral fusion and spread. *Cell Host Microbe* 16:736–747. <https://doi.org/10.1016/j.chom.2014.11.001>.
  30. Lazear HM, Govero J, Smith AM, Platt DJ, Fernandez E, Miner JJ, Diamond MS. 2016. A mouse model of Zika virus pathogenesis. *Cell Host Microbe* 19:720–730. <https://doi.org/10.1016/j.chom.2016.03.010>.
  31. Weber E, Finsterbusch K, Lindquist R, Nair S, Lienenkaul S, Gekara NO, Janik D, Weiss S, Kalinke U, Överby AK, Kröger A. 2014. Type I interferon protects mice from fatal neurotropic infection with Langkat virus by systemic and local antiviral responses. *J Virol* 88:12202–12212. <https://doi.org/10.1128/JVI.01215-14>.
  32. Schreier S, Cebulski K, Kröger A. 2021. Contact-dependent transmission of Langkat and tick-borne encephalitis virus in type I interferon receptor 1-deficient mice. *J Virol* 95:e02039–20. <https://doi.org/10.1128/JVI.02039-20>.
  33. Robertson SJ, Lubick KJ, Freedman BA, Carmody AB, Best SM. 2014. Tick-borne flaviviruses antagonize both IRF-1 and type I IFN signaling to inhibit dendritic cell function. *J Immunol* 192:2744–2755. <https://doi.org/10.4049/jimmunol.1302110>.
  34. Werme K, Wigerius M, Johansson M. 2008. Tick-borne encephalitis virus NS5 associates with membrane protein scribble and impairs interferon-stimulated JAK/STAT signaling. *Cell Microbiol* 10:696–712. <https://doi.org/10.1111/j.1462-5822.2007.01076.x>.
  35. Shi G, Schwartz O, Compton AA. 2017. More than meets the I: the diverse antiviral and cellular functions of interferon-induced transmembrane proteins. *Retrovirology* 14:1–11. <https://doi.org/10.1186/s12977-017-0377-y>.
  36. Narayana SK, Helbig KJ, McCartney EM, Eyre NS, Bull RA, Eltahla A, Lloyd AR, Beard MR. 2015. The interferon-induced transmembrane proteins, IFITM1, IFITM2, and IFITM3 inhibit hepatitis C virus entry. *J Biol Chem* 290:25946–25959. <https://doi.org/10.1074/jbc.M115.657346>.
  37. Raychoudhuri A, Shrivastava S, Steele R, Kim H, Ray R, Ray RB. 2011. ISG56 and IFITM1 proteins inhibit hepatitis C virus replication. *J Virol* 85:12881–12889. <https://doi.org/10.1128/JVI.05633-11>.
  38. Yount JS, Moltedo B, Yang Y-Y, Charron G, Moran TM, López CB, Hang HC. 2010. Palmitoylome profiling reveals S-palmitoylation-dependent antiviral activity of IFITM3. *Nat Chem Biol* 6:610–614. <https://doi.org/10.1038/nchembio.405>.
  39. John SP, Chin CR, Perreira JM, Feeley EM, Aker AM, Savidis G, Smith SE, Elia AEH, Everitt AR, Vora M, Pertel T, Elledge SJ, Kellam P, Brass AL. 2013. The CD225 domain of IFITM3 is required for both IFITM protein association and inhibition of influenza A virus and dengue virus replication. *J Virol* 87:7837–7852. <https://doi.org/10.1128/JVI.00481-13>.
  40. Zhao X, Sehgal M, Hou Z, Cheng J, Shu S, Wu S, Guo F, Le Marchand SJ, Lin H, Chang J, Guo J-T. 2018. Identification of residues controlling restriction versus enhancing activities of IFITM proteins on entry of human coronaviruses. *J Virol* 92:e01535–17. <https://doi.org/10.1128/JVI.01535-17>.
  41. Jia R, Pan Q, Ding S, Rong L, Liu S-L, Geng Y, Qiao W, Liang C. 2012. The N-terminal region of IFITM3 modulates its antiviral activity by regulating IFITM3 cellular localization. *J Virol* 86:13697–13707. <https://doi.org/10.1128/JVI.01828-12>.
  42. Wu W-L, Grotefend CR, Tsai M-T, Wang Y-L, Radic V, Eoh H, Huang I-C. 2017.  $\Delta 20$  IFITM2 differentially restricts X4 and R5 HIV-1. *Proc Natl Acad Sci U S A* 114:7112–7117. <https://doi.org/10.1073/pnas.1619640114>.
  43. Gómez-Herranz M, Nekulova M, Faktor J, Hernychova L, Kote S, Sinclair EH, Nenutil R, Vojtesek B, Ball KL, Hupp TR. 2019. The effects of IFITM1 and IFITM3 gene deletion on IFN $\gamma$ -stimulated protein synthesis. *Cell Signal* 60:39–56. <https://doi.org/10.1016/j.cellsig.2019.03.024>.
  44. Sattentau Q. 2008. Avoiding the void: cell-to-cell spread of human viruses. *Nat Rev Microbiol* 6:815–826. <https://doi.org/10.1038/nrmicro1972>.
  45. Savidis G, Perreira JM, Portmann JM, Meraner P, Guo Z, Green S, Brass AL. 2016. The IFITMs inhibit Zika virus replication. *Cell Rep* 15:2323–2330. <https://doi.org/10.1016/j.celrep.2016.05.074>.
  46. Perreira JM, Chin CR, Feeley EM, Brass AL. 2013. IFITMs restrict the replication of multiple pathogenic viruses. *J Mol Biol* 425:4937–4955. <https://doi.org/10.1016/j.jmb.2013.09.024>.
  47. Lindquist L, Vapalahti O. 2008. Tick-borne encephalitis. *Lancet* 371:1861–1871. [https://doi.org/10.1016/S0140-6736\(08\)60800-4](https://doi.org/10.1016/S0140-6736(08)60800-4).
  48. Sledz CA, Holko M, De Veer MJ, Silverman RH, Williams BR. 2003. Activation of the interferon system by short-interfering RNAs. *Nat Cell Biol* 5:834–839. <https://doi.org/10.1038/ncb1038>.
  49. Spence JS, He R, Hoffmann H-H, Das T, Thimon E, Rice CM, Peng T, Chandran K, Hang HC. 2019. IFITM3 directly engages and shuttles incoming virus particles to lysosomes. *Nat Chem Biol* 15:259–268. <https://doi.org/10.1038/s41589-018-0213-2>.
  50. Yount JS, Karssemeijer RA, Hang HC. 2012. S-palmitoylation and ubiquitination differentially regulate interferon-induced transmembrane protein 3 (IFITM3)-mediated resistance to influenza virus. *J Biol Chem* 287:19631–19641. <https://doi.org/10.1074/jbc.M112.362095>.
  51. Lannes N, Garcia-Nicolàs O, Démoulin T, Summerfield A, Filgueira L. 2019. CX3 CR1-CX3 CL1-dependent cell-to-cell Japanese encephalitis virus transmission by human microglial cells. *Sci Rep* 9:1–13.
  52. Yang C-F, Tu C-H, Lo Y-P, Cheng C-C, Chen W-J. 2015. Involvement of tetraspanin C189 in cell-to-cell spreading of the dengue virus in C6/36 cells. *PLoS Negl Trop Dis* 9:e0003885. <https://doi.org/10.1371/journal.pntd.0003885>.
  53. Sherer NM, Lehmann MJ, Jimenez-Soto LF, Horensavitz C, Pypaert M, Mothes W. 2007. Retroviruses can establish filopodial bridges for efficient cell-to-cell transmission. *Nat Cell Biol* 9:310–315. <https://doi.org/10.1038/ncb1544>.
  54. Tarr AW, Lafaye P, Meredith L, Damier-Piolle L, Urbanowicz RA, Meola A, Jestin J-L, Brown RJP, McKeating JA, Rey FA, Ball JK, Krey T. 2013. An alpaca nanobody inhibits hepatitis C virus entry and cell-to-cell transmission. *Hepatology* 58:932–939. <https://doi.org/10.1002/hep.26430>.
  55. Chmielewska AM, Naddeo M, Capone S, Ammendola V, Hu K, Meredith L, Verhoye L, Rychlowska M, Rappuoli R, Ulmer JB, Colloca S, Nicosia A, Cortese R, Leroux-Roels G, Balfe P, Bienkowska-Szewczyk K, Meuleman P, McKeating JA, Folgori A. 2014. Combined adenovirus vector and hepatitis C virus envelope protein prime-boost regimen elicits T cell and neutralizing antibody immune responses. *J Virol* 88:5502–5510. <https://doi.org/10.1128/JVI.03574-13>.
  56. Vendrame D, Sourisseau M, Perrin V, Schwartz O, Mammano F. 2009. Partial inhibition of human immunodeficiency virus replication by type I interferons: impact of cell-to-cell viral transfer. *J Virol* 83:10527–10537. <https://doi.org/10.1128/JVI.01235-09>.
  57. Richardson MW, Carroll RG, Stremlau M, Korokhov N, Humeau LM, Silvestri G, Sodroski J, Riley JL. 2008. Mode of transmission affects the sensitivity of human immunodeficiency virus type 1 to restriction by rhesus TRIM5 $\alpha$ . *J Virol* 82:11117–11128. <https://doi.org/10.1128/JVI.01046-08>.
  58. Jolly C, Booth NJ, Neil SJ. 2010. Cell-cell spread of human immunodeficiency virus type 1 overcomes tetherin/BST-2-mediated restriction in T cells. *J Virol* 84:12185–12199. <https://doi.org/10.1128/JVI.01447-10>.

59. Kuhl BD, Sloan RD, Donahue DA, Bar-Magen T, Liang C, Wainberg MA. 2010. Tetherin restricts direct cell-to-cell infection of HIV-1. *Retrovirology* 7: 115–113. <https://doi.org/10.1186/1742-4690-7-115>.
60. Sigal A, Kim JT, Balazs AB, Dekel E, Mayo A, Milo R, Baltimore D. 2011. Cell-to-cell spread of HIV permits ongoing replication despite antiretroviral therapy. *Nature* 477:95–98. <https://doi.org/10.1038/nature10347>.
61. Barretto N, Sainz B, Jr, Hussein S, Uprichard SL. 2014. Determining the involvement and therapeutic implications of host cellular factors in HCV cell-to-cell spread. *J Virol* 88:5050–5061. <https://doi.org/10.1128/JVI.03241-13>.
62. Mori K, Haruyama T, Nagata K. 2011. Tamiflu-resistant but HA-mediated cell-to-cell transmission through apical membranes of cell-associated influenza viruses. *PLoS One* 6:e28178. <https://doi.org/10.1371/journal.pone.0028178>.
63. Lipinska AD. 2006. Bovine herpesvirus 1 UL49. 5 protein inhibits the transporter associated with antigen processing despite complex formation with glycoprotein M. *J Virol* 80:5822–5832. <https://doi.org/10.1128/JVI.02707-05>.
64. Sanjana NE, Shalem O, Zhang F. 2014. Improved vectors and genome-wide libraries for CRISPR screening. *Nat Methods* 11:783–784. <https://doi.org/10.1038/nmeth.3047>.